

An Unprecedented Octadecanuclear Copper(II) Pyrazolate–Phosphonate Nanocage: Synthetic, Structural, Magnetic, and Mechanistic Study

Javeed Ahmad Sheikh, Himanshu Sekhar Jena, Amit Adhikary, Sajal Khatua, and Sanjit Konar*

Department of Chemistry, IISER Bhopal, Bhopal 462023, India

Supporting Information

ABSTRACT: A novel octadecanuclear copper pyrazolate–phosphonate nanocage with a bowl-shaped arrangement of the copper(II) centers in the asymmetric unit is reported. Characterization of intermediates in both solid and solution states aids to propose the mechanism of such a giant aggregation. Magnetic studies affirm the presence of antiferromagnetic interactions between the adjacent copper(II) centers. Extensive supramolecular interactions result in a framework structure.

The synthesis and characterization of polynuclear transition-metal cages and clusters has emerged as an active research area in the field of coordination chemistry, not only because of their architectural beauty¹ but also because of their immense technological applications² and relevance in biological systems.³ Numerous examples of transition-metal cages deliberating fascinating properties are found in the literature.^{4,5} However, the polynuclear copper(II) cages, in general, are relatively rare,⁶ and those based on phosphonates are scarce⁷ partly because of their limited solubility in most of the common solvents. Over the past few years, several transition-metal phosphonate cages have been reported by various groups to explore metal phosphonate cage compounds as magnetic materials.^{2a,b,4a,c,7,8} From a magnetic point of view, regular polygonal-type paramagnetic cores are extremely important and find wide applications.² As a part of our investigation into the exploration of cages with regular geometrical cores, recently we reported dodecanuclear and pentadecanuclear cobalt phosphonate cages featuring butterfly and distorted cubic cores, respectively.⁹ However, the majority of the phosphonate cages reported so far are formed by serendipitous assembly. Finding logical approaches for the inclusion of large numbers of metal ions having the expected geometrical arrangement is a big synthetic challenge that requires more mechanistic investigation.

Considering all of these facts, we planned to investigate the mechanistic details of cage formation by electrospray ionization mass spectrometry (ESI-MS) and structural study for an octadecanuclear copper(II) pyrazolate–phosphonate cage having the molecular formula $[\text{Cu}_{18}(\text{L})_8(\text{Pz})_{12}(\mu_2\text{-OH})_6(\mu_3\text{-OH})_2(\text{H}_2\text{O})_2(\text{Py})_4]\cdot 2\text{CH}_3\text{CN}\cdot 2\text{H}_2\text{O}$ (L = dianionic phenylphosphonate, Pz = pyrazolyl, and Py = pyridine). To the best of our knowledge, this is the first report of an investigation of the mechanism for a serendipitously assembled phosphonate cage. The title compound was obtained by the reaction of $\text{Cu}(\text{NO}_3)_2\cdot 2.5\text{H}_2\text{O}$, pyrazole, and *p*-methylphenylphosphonic acid¹⁰ (LH_2)

in a 2:1:1 ratio under ambient conditions in the presence of NET_3 and Py as shown in Scheme S1 in the Supporting Information (SI). Isolation of $[\text{Cu}_3(\text{Pz})_3(\mu_3\text{-OH})(\text{Py})_3(\text{NO}_3)_2]$ (**I**; Figure 2a) without the addition of a phosphonate ligand in the above reaction enabled us to propose the mechanism of this aggregation, as shown in Scheme S2 in the SI. The time-resolved ESI-MS spectra of intermediates **I** and **II** and asymmetric unit **III** (Scheme 1) further support the proposed mechanism. It is reasonable to assume that the $\mu_3\text{-OH}$ -bridged triangular Cu_3 core (**I**) of cage **1** is formed in the first step. Further, phosphonate ligands not only induce the expansion of **I** to a distorted hexagonal Cu_6 core (**II**) but also stitch both of them from the edges and center, resulting in intermediate **III**. This is further linked to a symmetry-related unit through one edge phosphonate ligand to give compound **1**.

Single-crystal X-ray analysis revealed that **1** crystallizes in the $\text{P}\bar{1}$ space group. The perspective view of **1** is displayed in Figure 1. This remarkable structural aggregation is due to the versatile coordination adaptability of the copper(II) ions in the presence of 8 dianionic phosphonate [L], 12 pyrazolyl (Pz), 6 $\mu_2\text{-OH}$, 2 $\mu_3\text{-OH}$, and 4 Py ligands. The core structure of **1** after removal of all of the carbon atoms for clarity is given in Figure S4 in the SI. The overall structure reveals an approximate chair shape (Figure S5 in the SI). The asymmetric unit of **1** contains a nonanuclear copper(II) core made of two subunits^{7a} [trinuclear (A) and hexameric (B)] tethered by a phosphonate ligand, giving a tortoise-like view (Figure 2b).

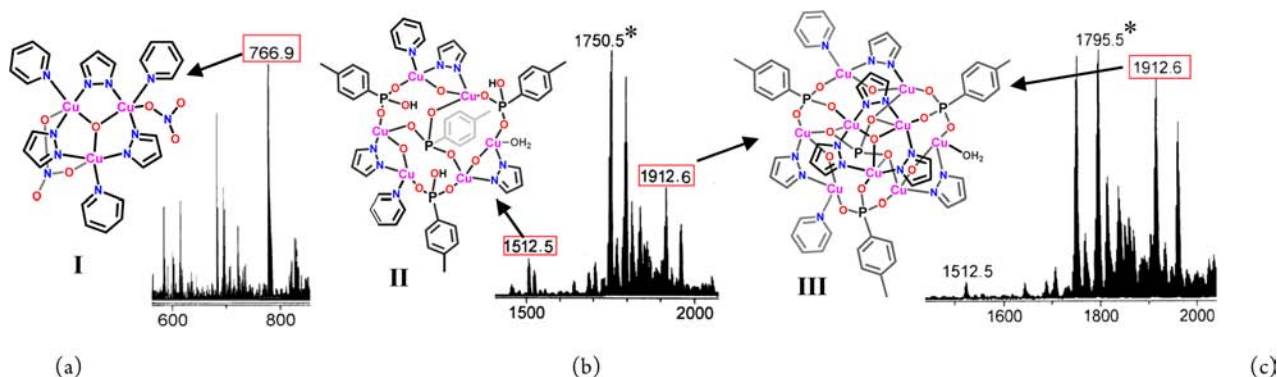
It is further interlinked to another Cu_9 cage via an edge phosphonate (P2) ligand in $[4.211]^{11}$ mode (Scheme S3 in the SI), giving a displaced Dawson structure¹² (Figure S6 in the SI). The upper rim (A) of the asymmetric unit contains three copper(II) centers in a triangular array to form a nine-membered $[\text{Cu-N-N}]_3$ metallacycle (Figure S7b in the SI), whereas the lower rim (B) contains six copper(II) centers in a distorted hexagonal array.

The center of the metallacycle in subunit A accommodates a pyramidal $\mu_3\text{-OH}$ group (O17) bridging nearly symmetrically to three copper(II) centers and is 0.440 Å out-of-plane of three copper centers (Cu3, Cu6, and Cu8). Similarly in subunit B, two adjacent copper(II) atoms are bridged by a pyrazolyl group, phosphonate oxygen, $\mu_2\text{-OH}$ groups, and Py in the periphery, which results in three contiguous puckered 10-membered $\text{Cu}_3\text{P}_2\text{O}_5$ rings, with phosphorus atoms significantly deviating

Received: July 8, 2013

Published: August 14, 2013



Scheme 1. ESI-MS Spectra Taken after (a) 5 min, (b) 30 min, and (c) 1 h^a

^aAsterisks: we were not able to assign these peaks. The intensity of the asymmetric unit peak increases with time. The full range of spectra are given in Figures S1–S3 in the SI.

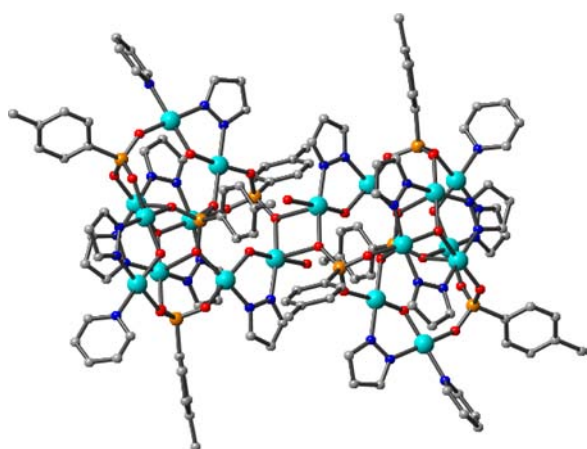


Figure 1. Ball-and-stick model representing the molecular structure of **1**. Color code: cyan, copper; orange, phosphorus; red, oxygen; gray, carbon; blue, nitrogen. Hydrogen atoms are omitted for clarity.

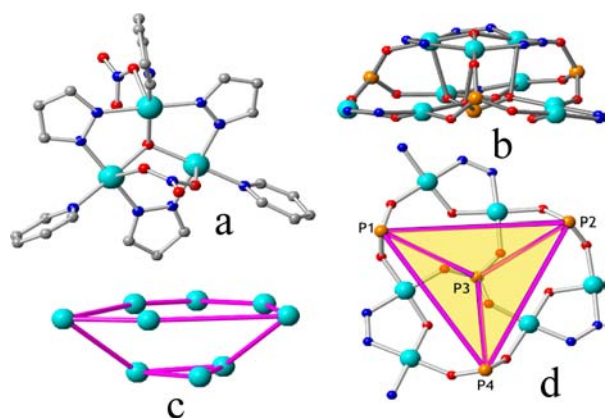


Figure 2. (a) Molecular structure of intermediate **1** (copper trimer). (b) Tortoise-like and (c) bowl-like views of the copper centers in the asymmetric unit. (d) Tetrahedral arrangement of phosphorus atoms. Color code: same as that in Figure 1.

from the mean plane of the ring (Figure S6b in the SI). Subunits A and B are stitched asymmetrically by four phosphonate ligands from three edges in [3.111]¹¹ coordination mode and one from the central side having a [6.222]¹¹ mode holding them together. The bond distances and angles around the copper(II) centers are listed in Table S1 in the SI. The Cu–Cu distances between two

adjacent copper(II) centers bridged by a μ_2 -pyrazolyl group and phosphonate ligands are ~ 3.3 and ~ 5.3 Å, respectively (Table S2 in the SI). The nine copper(II) centers in the asymmetric unit can be classified into four types depending on their coordination environment, geometry, and nature of ligation (Figure S8 in the SI). Two types of copper(II) centers in subunit B possess a coordination number of 4 [Cu2, Cu5, and Cu9 (1N, 3O); Cu1 and Cu4 (2N, 2O)] in a square-planar geometry; the other type observes a coordination number of 5 [Cu7 (1N, 4O)] in a distorted square-pyramidal geometry ($\tau = 0.1$).¹³ Another type of copper(II) center in subunit A are five-coordinated [Cu3 ($\tau = 0.14$), Cu6 ($\tau = 0.17$), and Cu8 ($\tau = 0.2$) (2N, 3O)] in a distorted square-pyramidal geometry. Connecting the nine copper centers in the asymmetric unit by imaginary lines results in a bowl shape (Figure 2c), where triangular copper(II) centers are present in the bottom, distorted hexagonal copper(II) centers at the top, and phosphonate oxygen atoms on the walls of the bowl. A similar analysis of phosphorus atoms of the phosphonate ligands reveals a tetrahedral arrangement of the same (Figure 2d). This type of fascinating structural arrangement is quite unique in phosphonate systems and has never been reported so far.

Another feature of **1** is the presence of intricate intramolecular hydrogen-bonding interactions between the μ -hydroxide group and the oxygen atoms of the phosphonate ligands in rim B, which might be a stabilizing force for such a hexanuclear moiety. Despite of the aforementioned hydrogen-bonding interactions, **1** also exhibits a wide variety of weak noncovalent interactions such as C–H \cdots O and C–H \cdots π (Table S3 in the SI) that assemble the discrete molecules to form a 2D framework, as illustrated in Figure S9 in the SI. Here all of the copper(II) atoms are organized in a staircase-like arrangement (Figure S10 in the SI). Further it is extended to a 3D framework by C–H \cdots π interactions, resulting in water channels (13.51 Å \times 17.88 Å) inside the framework down the *b* axis, as shown in Figure S11 in the SI. It was found that one of the lattice water molecules is exactly in the center of the channel, whereas the other hydrogen-bonded lattice water and acetonitrile molecules are near the wall of the channel.

For magnetic characterization, direct-current susceptibility data of **1** were collected on the polycrystalline sample in the range 1.8–300 K at 0.1 T. The magnetic measurement for **1** is shown in the form of a $\chi_M T$ (χ_M is the molar magnetic susceptibility) versus temperature (*T*) plot in Figure 3.

The room temperature $\chi_M T$ value for **1** (5.93 cm³ K mol⁻¹) is lower than the calculated spin-only value for isolated 18

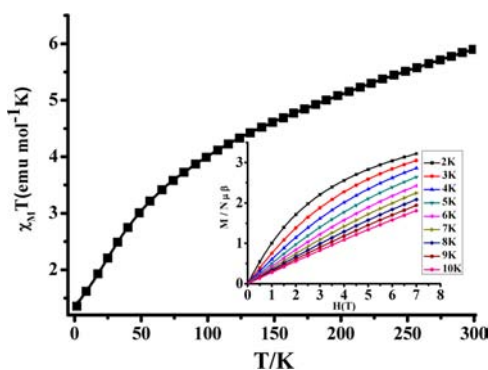


Figure 3. Temperature dependence of $\chi_M T$ measured at 0.1 T and magnetization curve (inset graphs) measured at 2–10 K for complex 1.

copper(II) centers ($6.75 \text{ cm}^3 \text{ K mol}^{-1}$; $g = 2$) because of dominant antiferromagnetic interactions. The $\chi_M T$ value decreases gradually from room temperature to $4.01 \text{ cm}^3 \text{ K mol}^{-1}$ at 98 K and then sharply to $1.35 \text{ cm}^3 \text{ K mol}^{-1}$ at 1.8 K. The above data were fitted with the Hamiltonian (see eq 1 and Figure S12 in the SI), which gives $g = 2.05$, $J_1 = -6.04 \text{ cm}^{-1}$, $J_2 = -135.23 \text{ cm}^{-1}$, $J_3 = 13.19 \text{ cm}^{-1}$, $J_4 = -20.04 \text{ cm}^{-1}$, and $J_5 = -1.85 \text{ cm}^{-1}$. Five exchange pathways can be seen clearly in the asymmetric unit (Figure S13 in the SI). Cu–O–Cu bond angles via J_1 and J_2 exchange pathways are $\sim 114^\circ$ and $\sim 122^\circ$, respectively; hence, antiferromagnetic interaction is expected through these pathways. However, the larger angle via J_2 than J_1 may result in more antiferromagnetic exchange in the former. All of the Cu–O–Cu bond angles via J_3 are $\sim 96^\circ$ and would result in ferromagnetic interactions.¹⁴ The exchange pathways via J_4 and J_5 would also yield antiferromagnetic interactions; however, the lesser value of J_5 can be justified by the large Cu–Cu distances for the same. Because of the complexity in the structure, the low-temperature experimental data did not fit well. The $M/N\mu_B$ versus H plot for 1 from 2 to 10 K (inset of Figure 3) shows a steady increase that reaches $4.02 \mu_B$ (calcd = $4.50 \mu_B$) at 7 T and 3 K without any saturation. These values are inconsistent with 18 uncoupled copper(II) ions because of strong antiferromagnetic coupling between the copper(II) centers. The unsaturated behavior of the plots can be explained by assuming strong magnetic anisotropy of the ions present with high nuclearity, resulting in many spin states populated at low temperature.¹⁵

In conclusion, a Cu_{18} nanocage has been assembled that displays the potential of phosphonate ligands to prepare giant molecular cages with fascinating structures, which should stimulate a more profound and systematic exploitation of their potential. Further work along these lines is in progress in our group.

ASSOCIATED CONTENT

Supporting Information

X-ray crystallographic data in CIF format, ESI-MS spectra, structures, PXRD patterns, space-filling models, a TGA plot, synthesis scheme, and tables of bond distances and angles, copper distances, and hydrogen-bonding parameters. This material is available free of charge via the Internet at <http://pubs.acs.org>.

AUTHOR INFORMATION

Corresponding Author

*E-mail: skonar@iiserb.ac.in.

Notes

The authors declare no competing financial interest.

ACKNOWLEDGMENTS

J.A.S. and A.A. acknowledge CSIR for their JRF fellowship. H.S.J. thanks the IISER Bhopal for a postdoctoral fellowship. S.K. thanks the DST, Government of India, and IISER Bhopal for generous financial and infrastructural support.

REFERENCES

- (1) (a) Müller, A.; Sarkar, S.; Shah, S. Q. N.; Bögge, H.; Schmidtman, Sh.; Sarkar, M.; Kögerler, P.; Hauptfleisch, B.; Trautwein, A.; Schünemann, V. *Angew. Chem., Int. Ed.* **1999**, *38*, 3238. (b) Kortz, U.; Müller, A.; Slagere, J.; Schnack, J.; Dalal, N. S.; Dressel, M. *Coord. Chem. Rev.* **2009**, *253*, 2315. and references cited therein. (c) Müller, A.; Todea, A. M.; Bögge, H.; Slagere, J. V.; Dressel, M.; Stammler, A.; Rusu, M. *Chem. Commun.* **2006**, 3066.
- (2) (a) Zheng, Y. Z.; Evagelista, M.; Tuna, F.; Winpenny, R. E. P. *J. Am. Chem. Soc.* **2012**, *134*, 1057. (b) Zheng, Y. Z.; Pineda, E. M.; Helliwell, M.; Winpenny, R. E. P. *Chem.—Eur. J.* **2012**, *18*, 4161. (c) Thompson, M. E. *Chem. Mater.* **1994**, *6*, 1168. (d) Sessoli, R.; Gatteschi, D.; Caneschi, A.; Novak, M. A. *Nature* **1993**, *365*, 141.
- (3) (a) Lee, S. C.; Holm, R. H. *Chem. Rev.* **2004**, *104*, 1135. (b) Taft, K. L.; Papaefthymiou, G. C.; Lippard, S. J. *Science* **1993**, *259*, 1302. (c) Theil, E. C.; Matzapetakis, M.; Liu, X. J. *J. Biol. Inorg. Chem.* **2006**, *11*, 803.
- (4) (a) Dearden, A. L.; Parsons, S.; Winpenny, R. E. P. *Angew. Chem., Int. Ed.* **2001**, *40*, 151. (b) Watton, S. P.; Fuhrmann, R.; Pence, L. E.; Caneschi, A.; Cornia, A.; Abbati, G. L.; Lippard, S. J. *Angew. Chem., Int. Ed.* **1997**, *36*, 2774. (c) Brechin, E. K.; Cador, O.; Caneschi, A.; Cadiou, C.; Harris, S. G.; Parsons, S.; Vonci, M.; Winpenny, R. E. P. *Chem. Commun.* **2002**, 1860.
- (5) Tasiopoulos, A. J.; Vinslava, A.; Wernsdorfer, W.; Abboud, K. A.; Christou, G. *Angew. Chem., Int. Ed.* **2004**, *43*, 2117.
- (6) (a) Murugesu, M.; Clerac, R.; Anson, C. E.; Powell, A. K. *Inorg. Chem.* **2004**, *43*, 7269. (b) Abedin, T. S. M.; Thompson, L. K.; Miller, D. O.; Krupicka, E. *Chem. Commun.* **2003**, 708. (c) Mohamed, A. A.; Burini, A.; Galassi, R.; Paglialunga, D.; Galn-Mascars, J.-R.; Dunbar, K. R.; Fackler, J. P., Jr. *Inorg. Chem.* **2007**, *46*, 2348. (d) Bai, Y. L.; Tangoulis, V.; Huang, R. B.; Zheng, L. S.; Tao, J. *Chem.—Eur. J.* **2009**, *15*, 2377.
- (7) (a) Chandrashekar, V.; Kigsley, S. *Angew. Chem., Int. Ed.* **2000**, *39*, 2320. (b) Chandrashekar, V.; Nagarajan, L. *Dalton Trans.* **2009**, 6712. (c) Chandrashekar, V.; Senapati, T.; Dey, A.; Hossain, S. *Dalton Trans.* **2011**, *40*, 5394 and references cited therein.
- (8) (a) Breeze, B. A.; Shanmugam, M.; Tuna, F.; Winpenny, R. E. P. *Chem. Commun.* **2007**, 5185. (b) Konar, S.; Bhuvanesh, N.; Clearfield, A. *J. Am. Chem. Soc.* **2006**, *128*, 9604. (c) Konar, S.; Clearfield, A. *Inorg. Chem.* **2008**, *47*, 3489. (d) Konar, S.; Clearfield, A. *Inorg. Chem.* **2008**, *47*, 5573. (e) Beavers, C. M.; Prosser, A. V.; Cashion, J. D.; Dunbar, K. R.; Richards, A. F. *Inorg. Chem.* **2013**, *52*, 1670. (f) Murugavel, R.; Gogoi, N.; Clerac, R. *Inorg. Chem.* **2009**, *48*, 646.
- (9) Sheikh, J. A.; Goswami, S.; Adhikary, A.; Konar, S. *Inorg. Chem.* **2013**, *52*, 4127.
- (10) Bennett, J. A.; Hope, E. G.; Singh, K.; Stuart, A. M. *J. Fluorine Chem.* **2009**, *130*, 615.
- (11) Coxall, R. A.; Harris, S. G.; Henderson, D. K.; Parsons, S.; Tasker, P. A.; Winpenny, R. E. P. *J. Chem. Soc., Dalton Trans.* **2000**, 2349.
- (12) Müller, A. *Nature* **1991**, *352*, 115.
- (13) Addison, A. W.; Rao, T. N.; Reedijk, J.; Van Rijn, J.; Verschor, G. C. *J. Chem. Soc., Dalton Trans.* **1984**, 1349.
- (14) Kahn, O. *Molecular Magnetism*; VCH: New York, 1993.
- (15) Ma, Y. S.; Song, Y.; Tang, X. Y.; Yuan, R. X. *Dalton Trans.* **2010**, 39, 6262.